Scilight

Nano-electrochemistry & Nano-photochemistry

https://www.sciltp.com/journals/nenp

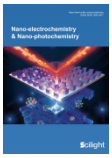

Check for updates

Article

Smartphone-Based Electrochemiluminescence Sensors

Fangxin Du *, Nana You, Xiaoping Hu, Fuli Xu and Gen Liu *

Key Laboratory of Green and Precise Synthetic Chemistry and Applications, Ministry of Education; School of Chemistry and Chemical Engineering, Huaibei Normal University, Huaibei 235000, China

* Correspondence: dufx@chnu.edu.cn (F.D.); liugen7084@126.com (G.L.)

How To Cite: Du, F.; You, N.; Hu, X.; et al. Smartphone-Based Electrochemiluminescence Sensors. *Nano-electrochemistry & Nano-photochemistry* **2026**, *2*(3), 16. https://doi.org/10.53941/nenp.2026.100016

Received: 14 May 2026

Revised: 12 June 2026

Accepted: 22 June 2026

Published: 14 July 2026

Abstract: Electrochemiluminescence (ECL) represents a unique optical-electrochemical transduction mechanism with high sensitivity, low background noise, and excellent controllability. However, conventional ECL systems rely on bulky, expensive laboratory instruments, severely limiting their application in point-of-care testing (POCT) and resource-limited scenarios. The integration of smartphones, with their high-performance processors, high-resolution cameras, programmable light sources, and wireless communication modules, has opened a new avenue for miniaturized, portable, and intelligent ECL sensing. This review systematically summarizes the fundamental principles of smartphone-based ECL detection, including ECL luminescence mechanisms, electrode configurations, and smartphone module integration. The latest advances in representative applications of smartphone ECL technology in bioanalysis, environmental monitoring, and food safety are comprehensively overviewed. Particular attention is paid to the auxiliary role of artificial intelligence, specifically the differentiated contributions of traditional machine learning algorithms for small-sample spectral feature analysis and deep learning architectures for high-dimensional imaging data processing, and machine learning in solving core challenges such as weak signal detection, background interference, and quantitative accuracy improvement. Finally, current limitations and future development directions toward fully integrated, self-powered, and intelligent ECL platforms are discussed, aiming to provide a systematic reference for the practical translation of this technology.

Keywords: electrochemiluminescence; smartphone; artificial intelligence; point-of-care testing

1. Introduction

Electrochemiluminescence (ECL) is a luminescence process driven by electrochemical reactions at the electrode-electrolyte interface, where electron transfer generates high-energy excited species that emit light upon returning to the ground state [1]. Distinguished from fluorescence, chemiluminescence, and other optical detection techniques, ECL exhibits outstanding merits including ultrahigh sensitivity, strong selectivity, negligible background interference, and superior controllability. These advantages render ECL an indispensable analytical tool for clinical diagnosis, environmental monitoring, and food safety [2–5]. However, conventional ECL detection relies on large and expensive analytical instruments, which require professional operation, complex supporting equipment, and fixed laboratory environments, greatly limiting its application in field testing, emergency detection, and resource-limited areas.

With the rapid development of mobile communication, microelectronics, and intelligent imaging technology, smartphones have evolved into portable multifunctional platforms integrating high-performance processors, high-resolution complementary metal oxide semiconductor (CMOS) cameras, controllable flash modules, stable power supply and wireless communication modules. These features are highly compatible with the development goals of

miniaturized, intelligent, and portable ECL systems, providing a universal and low-cost strategy to break the application bottlenecks of traditional ECL technology. The integration of smartphones and ECL detection has realized the transformation of ECL analysis from laboratory professional equipment to point-of-care testing (POCT) devices, enabling real-time, on-site, and low-cost quantitative detection, and showing great application potential in rapid screening, on-site monitoring, and emergency detection [6–9]. Since 2020 [10], intelligent algorithm-assisted strategies have been increasingly adopted in smartphone-based ECL sensing, which effectively improve signal identification accuracy, suppress background interference, optimize quantitative calibration, and significantly enhance the intelligence and reliability of portable detection systems [11–14].

Against this background, this review focuses on the research progress of smartphone-integrated ECL sensors from 2020 to 2026. The fundamental principles, including ECL generation mechanisms, electrode configuration characteristics, and smartphone module integration strategies, are systematically elaborated. Representative applications of smartphone-based ECL technology in bioanalysis, environmental monitoring, and food safety are comprehensively summarized. Meanwhile, the auxiliary roles and implementation pathways of artificial intelligence algorithms in ECL image processing, signal denoising, multi-signal decoupling, and high-precision quantification are highlighted. Finally, the current challenges in this field are analyzed, and the future development directions, including system integration, miniaturization design, intelligent algorithm optimization, and multi-technology fusion, are prospected. This review is expected to provide a systematic theoretical reference and practical guidance for researchers in related fields and further promote the development and practical transformation of smartphone ECL detection technology.

2. Fundamentals of Smartphone ECL Detection

The core principle of smartphone-based ECL detection includes two key components: the fundamental mechanism of ECL generation and the integration principle of portable smartphone detection modules. According to the reaction pathway, ECL can be divided into annihilation ECL and co-reactant ECL. Annihilation ECL relies on electron transfer between oxidized and reduced intermediates of the same luminophore, whereas co-reactant ECL involves electrochemical reactions between luminophores and co-reactants to produce excited emitters. Owing to their high luminous efficiency, stable signal output, and simple operation, co-reactant ECL systems based on various nanomaterials, such as metal-organic frameworks (MOFs) [15,16], graphitic carbon nitride (g-C_3N_4), and quantum dots (QDs) [17–19], have become the mainstream strategy for quantitative analysis in smartphone-assisted portable sensing platforms.

Electrode devices provide indispensable reaction sites for electrochemical redox and excited-state generation, which directly determine the stability and reliability of ECL signals. Three typical configurations are widely adopted in smartphone ECL platforms: single-electrode electrochemical system (SEES), bipolar electrode (BPE) system, and three-electrode system. SEES employs only one conductive electrode to drive both anodic and cathodic reactions simultaneously, featuring an ultra-simple, miniaturized, wireless-compatible structure ideal for portable and disposable smartphone-integrated detection [20–25]. BPE consists of a wirelessly powered conductive sheet, where anodic and cathodic reactions occur separately at two poles under an external electric field, enabling wireless ECL imaging suitable for integrated miniaturized devices [26–29]. The three-electrode system, composed of a working electrode, reference electrode, and counter electrode, remains the most robust and accurate configuration, and its screen-printed miniaturized format can be readily integrated with smartphone-based portable platforms [30–32]. Notably, a distinctive self-powered ECL system has been developed using galvanized iron that acts as both power source and working electrode, enabling wireless, battery-free ECL imaging and quantitative analysis without any external power supply [33]. It relies on the spontaneous galvanic reaction between the zinc coating (standard electrode potential: −0.76 V vs. SHE) and the iron substrate (standard electrode potential: −0.44 V vs. SHE) to generate a driving potential for ECL, eliminating the need for external power and thus reducing device size and cost. With an ultra-simplified structure, no requirement for peripheral power modules, and compatibility with disposable detection chips, it is highly suitable for field testing in resource-limited regions. The primary limitation lies in its fixed output potential, which cannot be flexibly tuned for different ECL systems, and the gradual decay of driving voltage as the zinc coating corrodes, leading to signal drift during long-term detection. Currently, the system supports smartphone-based corrosion imaging and ascorbic acid detection with a linear range of 0.5–100 μM and a limit of detection (LOD) of 0.31 μM.

The effective integration of smartphone modules is essential for realizing portable, visual, and intelligent ECL analysis. In a typical smartphone-based POCT platform [34], the built-in high-resolution CMOS camera serves as the core optical detector, allowing ECL images to be captured in a dark or light-shielded microenvironment (Figure 1). Where necessary, the smartphone's flash can also provide auxiliary excitation for

certain ECL systems. To quantify target analytes, custom-developed mobile applications or image analysis algorithms are used to extract features such as luminescence intensity, grayscale values, RGB/HSV parameters, and region-of-interest signals, establishing reliable calibration curves [35,36]. Two key technical challenges in smartphone integration are addressed: matching the typically weak ECL signals with the camera's sensitivity through optimized exposure time and gain settings, and minimizing ambient light interference via enclosed dark chambers and refined imaging parameters. Moreover, smartphones can directly supply stable power to the electrochemical system or cooperate with near-field communication-based passive energy harvesting, enabling compact, battery-free, and fully integrated portable ECL detection platforms.

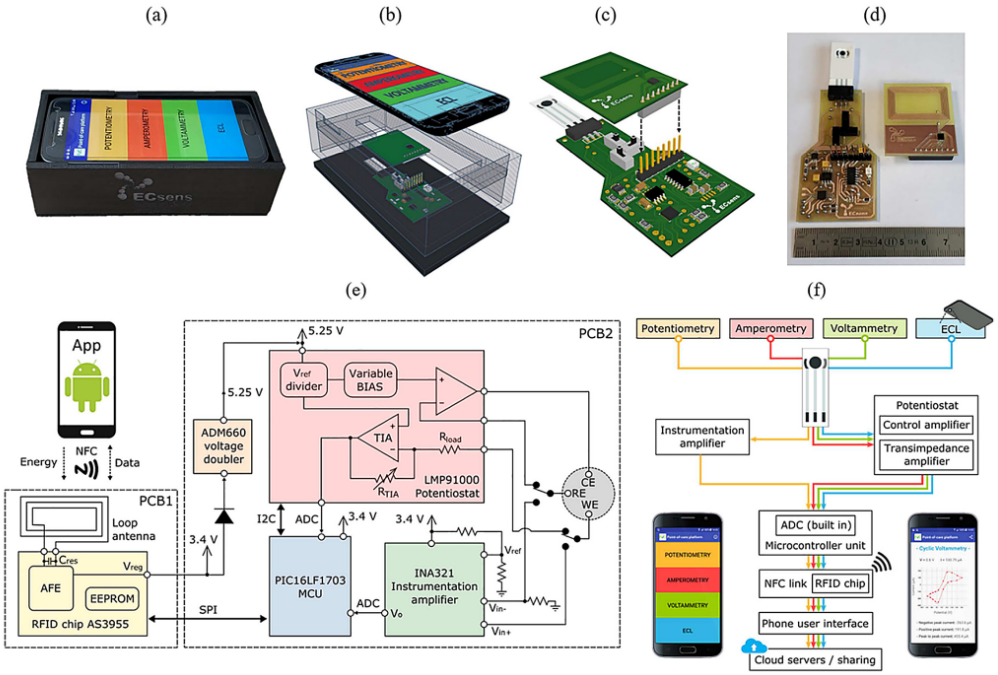

Figure 1. Smartphone-based analytical platform: (**a**,**b**) photos and exploded view of the full device with light-shielding holder; (**c**,**d**) printed circuit board (PCB) design and photograph with screen-printed electrode (SPE); (**e**) PCB power/data flow; (**f**) system block diagram and custom app interface for amperometry, potentiometry, cyclic voltammetry, and ECL [34]. Copyright 2019, Elsevier.

3. Intelligent Algorithm-Assisted Strategies for Smartphone-based ECL Detection

In the field of data analysis for ECL sensing, artificial intelligence (AI) has emerged as a powerful tool, with machine learning serving as its core branch. Machine learning algorithms can be broadly divided into traditional machine learning and deep learning methods. Traditional machine learning models, such as support vector machine (SVM) and random forest (RF), have been widely applied for classification, regression, and feature selection in ECL spectral and sensing data analysis, particularly excelling in handling small sample sizes and high-dimensional feature sets [10,14]. Deep learning, a subset of machine learning based on artificial neural networks (ANNs), offers stronger capabilities for modeling complex non-linear relationships in large datasets. As the fundamental form of ANN, the feedforward neural network (FNN, also known as multi-layer perceptron, MLP) realizes unidirectional data transmission from the input layer through hidden layers to the output layer with fully connected neurons between adjacent layers. Its multi-hidden-layer variant, deep neural network (DNN), and convolutional neural network (CNN), a specialized ANN with convolutional layers for local feature extraction, are two dominant deep learning architectures which both extensively used for quantitative prediction and pattern recognition in ECL-based biosensing [11–13,37–42]. The choice of algorithm should align with the dimensionality and modality of ECL data. Traditional machine learning models, including SVM and RF, are preferentially adopted for low-dimensional, structured spectral or electrochemical response data. These algorithms exhibit strong generalization performance with limited sample sizes and low computational overhead, rendering them ideal for lightweight on-site deployment on smartphone platforms. In contrast, deep learning architectures represented by CNN and DNN are better suited for high-dimensional, unstructured imaging data. Their multi-layer nonlinear mapping capability enables efficient extraction of spatial luminescence features and effective suppression of background noise, which is critical for the interpretation of complex visual signals.

As shown in Figure 2a,b, RF and FNN were adopted to fuse ECL imaging signals and amperometric responses in a typical $Ru(bpy)_3^{2+}$/TPrA ECL system equipped with screen-printed electrodes, establishing a nonlinear mapping between multi-dimensional signals and analyte concentration, thus improving the reliability of quantitative detection [10]. Additionally, a high-throughput ECL immunoassay platform based on a microcolumn array employed SVM and backpropagation neural networks to analyze RGB luminescence features, enabling sensitive and reliable detection of SARS-CoV-2 with a linear range of 0.001–10 ng mL^{-1} and a LOD as low as 0.86 pg mL^{-1}, while effectively reducing cross-contamination and signal interference [14]. Benefiting from low computational complexity and rapid processing speed, machine learning is highly suitable for lightweight on-site data analysis on smartphone-based ECL devices.

Alongside these methods, DNNs have been adopted to analyze the intricate connections between ECL signals and target analytes. For example, DNN-assisted multiparameter prediction was applied to a multicolor ECL detection array based on wavelength-tunable emissions from g-CN@Ag nanocomposites, enabling highly accurate dopamine quantification with a linear range of 0.1 nM to 1 mM and a LOD of 44 pM [18]. In contrast to structured spectral data analysis, convolutional neural networks (CNNs) excel at extracting spatial features from ECL imaging data. For 2,4-dichlorophenoxyacetic acid (2,4-D) analysis, a smartphone-integrated MIP ratiometric ECL sensor using Te-doped CdS@Mn_3O_4 and Luminol as dual emitters adopted CNN-based image processing to realize intelligent signal recognition and self-calibrated quantitative detection with excellent anti-interference capacity [12]. Similarly, in a dual-potential ECL system for tyramine (TYM) detection, CNN-assisted image analysis was utilized to synchronously process cathodic and anodic signals, expanding the linear range to 0.01–1000 μM and lowering the detection limit to 0.005 μM (Figure 2c) [39]. Building on general CNN architectures, custom-designed lightweight networks have been developed to meet the specific needs of rapid and field-deployable ECL sensing. For instance, a fast ECL judgment network (FEJ-Net) was applied to a ratiometric ECL sensor constructed from CdZnS/$SnIn_4S_8$ heterojunctions and Co_3O_4/CuO nanozymes, enabling intelligent analysis of dual-emission signals for the detection of tetracycline with high sensitivity and stability [42]. FEJ-Net was also integrated into a MIP-ECL platform utilizing oxygen vacancy-rich Tb@Lu_2O_3 nanoemitters, where it efficiently processes luminescence images to achieve ultrasensitive detection of ciprofloxacin [40].

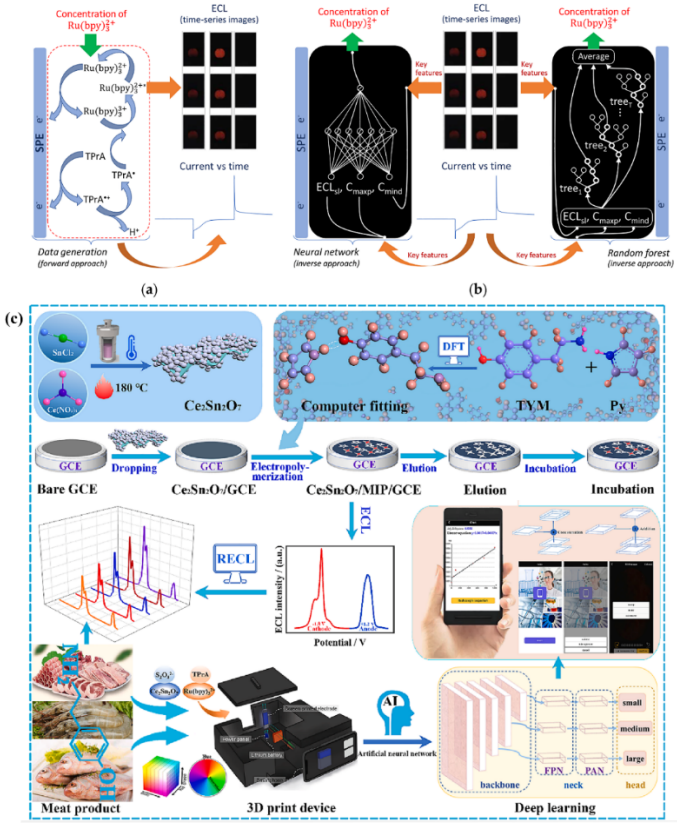

Figure 2. Schematic diagrams of (**a**) the procedure for experimental data generation (forward approach) using the mobile phone-based ECL sensor and (**b**) data-driven modeling (inverse approach) using a feedforward neural network and a random forest [10], Copyright 2020, MDPI, and (**c**) the construction of machine learning assisted smartphone-based visual and portable intelligent detection of TYM in agro-food products using $Ce_2Sn_2O_7$/MIP/GCE [39], Copyright 2023, Elsevier.

Collectively, these representative smartphone-coupled ECL assays, as systematically summarized in Table 1, demonstrate how different machine learning and deep learning models have been tailored to enhance detection performance, including expanded linear ranges, lowered limits of detection, and improved anti-interference capabilities across diverse analytes. The development of intelligent algorithm-assisted strategies in smartphone ECL detection is moving toward more compact, lightweight, and application-specific neural network designs, which not only enable real-time on-site analysis but also improve the reliability and portability of ECL sensing devices, paving the way for widespread deployment in food safety, environmental monitoring, and POCT scenarios.

Table 1. Smartphone-coupled ECL assays assisted with intelligent algorithm strategies.

Target	ECL System	Intelligent Algorithm	Linear Range	LOD	Ref.
$Ru(bpy)_3^{2+}$	$Ru(bpy)_3^{2+}$/TPrA	RF FNN	0.02–2.5 μM	0.02 μM	[10]
Furosemide	CdS QDs/$K_2S_2O_8$	CNN	0.01–100 μM	4 nM	[11]
2,4-D	Te-CdS@Mn_3O_4/H_2O_2 Luminol/H_2O_2	CNN	1 nM–100 μM	0.63 nM	[12]
Lactate	Luminol/H_2O_2	CNN	50–2000 μM	5.14 μM	[13]
SARS-CoV-2	Luminol/H_2O_2	SVM	0.001–10 ng mL^{-1}	0.86 pg mL^{-1}	[14]
DA	g-CN@Ag/$K_2S_2O_8$	DNN	0.1 nM–1 mM	44 pM	[18]
TYM	$Ce_2Sn_2O_7$/$K_2S_2O_8$ $Ru(bpy)_3^{2+}$/TPrA	CNN	0.01–1000 μM	0.005 μM	[39]
Ciprofloxacin	Tb@Lu_2O_3/$K_2S_2O_8$	FEJ-Net	5×10^{-4}–5×10^{2} μM	0.095 nM	[40]
Chlortetracycline	CdZnTeS/$K_2S_2O_8$	DNN	0.05–100 μM	0.029 μM	[41]

4. Applications of Smartphone ECL Detection

4.1. Bioanalysis

Bioanalysis is one of the most important application fields of smartphone ECL detection technology, with broad prospects in clinical diagnosis, POCT, and biological research. This technology has been widely used in the detection of various biological analytes, including small biological molecules, proteins, and nucleic acids, relying on its advantages of high sensitivity, high selectivity, portability, and rapidity.

4.1.1. Small Molecules

The portable detection of small-molecule biomarkers is crucial for early diagnosis, disease monitoring, and personalized therapy. Smartphone-based ECL sensors demonstrate immense potential for the quantitative detection of diverse small-molecule targets, owing to their high sensitivity and portability. In the realm of neurotransmitter detection, dopamine (DA) represents a classic and vital target. To realize its portable and accurate quantification, researchers have constructed a series of smartphone-integrated ECL platforms with progressive performance improvements. For instance, Zhu et al. [43] developed a fully integrated handheld ECL device consisting of a flexible printed circuit board electrochemical module, a silicon photomultiplier, and a Bluetooth-connected smartphone. Based on the ECL quenching effect of DA on the $Ru(bpy)_3^{2+}$/TPrA system, this device enabled sensitive DA detection in urine and rat brain homogenate with an LOD of 3.5 nM, showing strong potential for POCT in complex biological matrices. Similarly, Bhaiyya et al. [44] further proposed a 3D-printed closed BPE-ECL device based on the same $Ru(bpy)_3^{2+}$/TPrA system, realizing quantitative DA detection with a linear range of 0.5–100 μM and an LOD of 2 μM with smartphone- or IoT-assisted signal acquisition supporting real-time testing. To address high-throughput needs, Pan et al. [45] designed a position-resolved single-electrode ECL chip and a matching portable smartphone analyzer, which achieved high-throughput DA quantification with accuracy comparable to that of HPLC-MS/MS in serum samples.

Metabolite and disease biomarker detection constitutes another significant direction. Monitoring glucose is vital for diabetes management. Calabria et al. developed a 3D-printed smartphone ECL enzymatic biosensor employing a two-electrode configuration with carbon black-doped polylactic acid electrodes. By pre-loading Luminol and glucose oxidase into an agarose hydrogel matrix, they constructed a reagent-free sensor for selective glucose detection with an LOD of 60 μM, successfully applying it to artificial serum analysis [46]. In contrast, Wang et al. [47] constructed a CeO_2:Eu^{3+} nanozyme-based ECL-colorimetric dual-modal sensor for glucose. This nanomaterial exhibited excellent ECL performance with $K_2S_2O_8$ as a co-reactant, and its ECL intensity was effectively quenched by H_2O_2 generated from glucose oxidation, enabling highly sensitive detection with an

impressively low ECL-mode LOD of 0.033 nM. Galactose detection is significant for newborn galactosemia screening. Nie et al. [48] developed an innovative co-reactant modifier amplification ECL sensing method using nitrogen QDs for the portable diagnosis of galactose, with a linear range of 0.5 μM to 15 mM, an LOD of 0.16 μM, and successful application in spiked human serum samples.

Detection of other bioactive small molecules has also been reported. Adenosine triphosphate (ATP) serves as the universal currency of cellular energy. Nie et al. developed an ECL biosensor based on Fe_3O_4 NP@ZIF-8/MoS_2 QDs, incorporating a nanosurface energy transfer strategy. Using a smartphone to capture ECL imaging, they achieved portable ATP detection with a linear range of 0.05–200 nM and an LOD of 0.015 nM [49]. On this basis, Zhang et al. [50] further constructed an ATP aptasensor using L-cysteine-regulated polydopamine nanoparticles combined with an inner filter effect, achieving an ultra-low LOD of 3.79 fM with clear smartphone-based ECL imaging, further expanding the application of visual ECL analysis for ATP. Colchicine (COL) has a narrow therapeutic window requiring precise monitoring. Wu et al. [51] synthesized tegular carbon nitride nanosheets with a thickness of only 1.5 nm and combined them with molecularly imprinted polymers to construct a novel ECL sensor. Utilizing their self-developed smartphone-based ECL imaging device to guide sensor surface modulation, they reduced the LOD by four orders of magnitude, significantly improving COL sensing performance. Through regulation with o-fluorobenzoic acid, Li et al. [17] constructed porous graphitic carbon nitride with nitrogen defects capable of generating tunable multicolor ECL emission from 465 nm to 550 nm. For the first time, they established a smartphone-based multicolor ECL array and realized the discrimination of five polyphenols via principal component and hierarchical cluster analyses.

4.1.2. Proteins

Tumor marker proteins have been extensively explored as typical analytes in portable ECL platforms. A smartphone-based molecular imprinting (MIP) ECL microscope was constructed for the visual quantitation of alpha-fetoprotein (AFP) in saliva, utilizing a gold nanorods@polyethyleneimine@ferrocene (AuNRs@PEI@Fc) composite as a dual-mechanism quencher and $Ru(bpy)_3^{2+}$ as the emitter, achieving an ultra-low detection limit of 4.5 fg mL^{-1} for non-invasive liver cancer screening [52]. For carcinoembryonic antigen (CEA) detection, Shan-Shan Shi and colleagues [53] reported a smartphone-based POCT platform using Zr_6MOFs loaded with Fc-DNA as signal amplifiers, as illustrated in Figure 3. This platform achieved an LOD of 0.33 pg mL^{-1} and showed reliable performance in human serum, demonstrating potential for on-site cancer biomarker screening. In addition, a subsequent smartphone-compatible ECL biosensing platform leveraged Fe-Co-CeO_2@$Ti_3C_2(OH)_2$ heterostructures with rich oxygen vacancies and FeCo-NH_2-BDC as dual signal-amplifying probes for CEA detection, delivering an LOD of 12.42 pg mL^{-1} over a linear range of 35 pg mL^{-1} to 50 ng mL^{-1}, further expanding the scope of portable clinical screening [54].

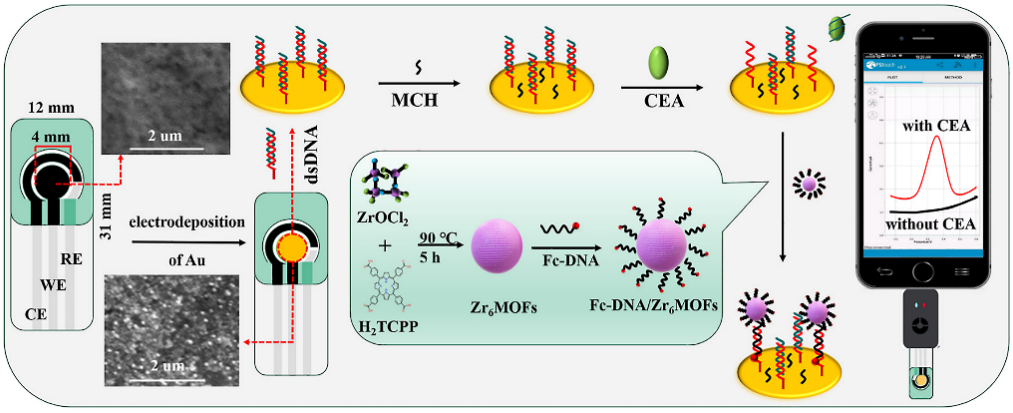

Figure 3. Schematic illustration of smartphone-based ECL sensing platform for CEA detection [53]. Copyright 2024, Royal Society of Chemistry.

Viral and pathogenic proteins have also been accurately detected via smartphone-assisted ECL strategies, which is highly desirable for rapid on-site screening of infectious diseases and health risks. A smartphone-integrated self-enhanced ECL array chip was developed for the label-free detection of SARS-CoV-2 nucleocapsid protein, utilizing Ru/PEI@SiO_2 nanocomposites as ECL emitters and a SEES to enhance portability, achieving a low detection limit of 0.47 pg mL^{-1} within a linear range of 1–10,000 pg mL^{-1} [55]. Beyond tumor and pathogenic antigens, smartphone-integrated ECL platforms have been successfully applied to the detection of cardiac disease-

related biomarkers and functional enzymes. By integrating NH_2-MIL-88 metal-organic frameworks that encapsulate tetraphenylethylene aggregation-induced emission molecules as nanoconfined catalytic reactors, a smartphone-adopted aggregation-induced ECL (AIECL) imaging system was designed, enabling intelligent, accurate, and on-site analysis of cardiac troponin I (cTnI) with enhanced local reactive species concentrations [15]. Furthermore, A CuInZnS QDs-based ECL sensor was developed for the visual detection of superoxide dismutase (SOD), where SOD competitively consumes hydrogen peroxide to quench the QD ECL signal, achieving a low detection limit of 0.03 μg mL^{-1}, supporting portable SOD monitoring in human blood samples [56].

4.1.3. Nucleic Acids

Nucleic acid detection, including DNA, microRNA (miRNA), and gene methylation analysis, is a cornerstone of clinical diagnosis, cancer screening, and infectious disease monitoring, and smartphone-integrated ECL sensing has emerged as a powerful, portable solution for this purpose. A ratiometric and enzyme-free ECL sensing platform was constructed for BRAF gene detection, utilizing sulfur-regulated boron nitride QDs as luminophores and an amplified surface plasmon-coupled ECL (SPC-ECL) strategy with gold nanoparticles; the system achieved a detection limit of 0.3 pM over a linear range of 1 pM to 1.5 nM, with ECL signals directly observable via smartphone imaging for portable on-site analysis [57]. For HPV 16 DNA detection, a high-efficiency ECL sensor was developed based on Zn-doped MoS_2 QDs with sulfur vacancies and reductive Cu(I) particles as catalytic signal amplifiers, integrated with a DNA walker amplification cycle. The biosensor realized sensitive detection from 0.1 nM to 200 nM with a LOD of 0.03 nM, and the entire battery-powered system was compatible with smartphone imaging for POCT [58].

For miRNA detection, multiple smartphone-assisted ECL strategies have been developed to achieve ultra-sensitive analysis. A polydopamine nanoparticles (PDA NPs) @MoS_2 nanosheet aerogel ECL sensing system was designed, where the aerogel prevented nanoparticle aggregation and facilitated electron transfer to amplify ECL signals by over 60 times; combined with a target-catalyzed hairpin assembly (CHA) sensing mode, the platform achieved visual detection of miRNA-126 with an ultra-low LOD of 0.56 aM, and the bright ECL emission was clearly captured by a smartphone [59]. Although this LOD demonstrates exceptional sensitivity in standard buffers, further optimization regarding anti-interference capabilities in complex biological matrices is required. In addition, two $Ru(bpy)_3^{2+}$-based MOF ECL biosensors were established for miRNA-21 detection with smartphone-assisted readout. One employed 3D zinc oxalate MOFs to confine $Ru(bpy)_3^{2+}$ chromophores and magnetic beads for dual signal amplification, enabling detection from 1.56 to 100 nM [60], while the other used $Ru(bpy)_2(L)^{4+}$@MOF-5 with nucleic acid cycle amplification and ferrocene-mediated signal quenching, achieving an extremely low LOD of 7.2 fM over a linear range of 1.0×10^{-14} to 1.0×10^{-9} M [61].

Beyond single nucleic acid targets, a closed split bipolar electrochemistry ECL system was developed for the visual one-step simultaneous detection of RASSF1A and SLC5A8 gene promoter methylation in papillary thyroid cancer. The system utilized Luminol -loaded Fe_3O_4@UiO-66 and AuNRs@C_3N_4 NS as ECL emitters on BPEs. With ECL signals recorded by a smartphone camera, it achieved discrimination of methylation levels as low as 0.01% with over 90% clinical sensitivity in patient plasma samples, enabling early cancer diagnosis and therapeutic response monitoring [62]. Collectively, these advances demonstrate that smartphone-integrated ECL sensing, combined with nanomaterial signal amplification, nucleic acid amplification strategies, and portable imaging, provides a versatile, sensitive, and user-friendly platform for nucleic acid detection in clinical and portable settings.

4.2. Environmental and Food Safety

Environmental and food safety monitoring represents a critical application domain for smartphone-integrated ECL sensing, enabling on-site, rapid, and sensitive detection of heavy metal ions, mycotoxins, antibiotic residues, and pesticide residues in complex matrices. In heavy metal detection, smartphone-coupled ECL strategies have enabled rapid, field-deployable monitoring of heavy metal ions and environmental pollutants including Hg^{2+}, Cu^{2+}, and Cr^{4+} [63–65]. For example, a dual-modal ECL-colorimetric sensor was established for Hg^{2+} analysis in environmental water using $Ru(dcbpy)_3^{2+}$-functionalized metal-polydopamine frameworks and thymine-rich DNA probes, achieving an ultralow detection limit of 0.32 pM with smartphone-assisted visual readout [64].

For mycotoxin analysis, a suite of innovative smartphone-compatible ECL platforms has been developed to tackle foodborne hazards. A closed BPE array ECL aptasensor was engineered for aflatoxin M1 (AFM1) detection in milk, where Luminol -functionalized silver nanoparticle-decorated graphene oxide served as signal tags; the smartphone-based readout delivered a linear response across 10–200 ng mL^{-1} with a LOD of 0.05 ng mL^{-1}, alongside exceptional reproducibility in complex dairy matrices [66]. To further enhance sensitivity, a dual-mode

colorimetric-ECL aptasensor was constructed for aflatoxin B1 (AFB1) screening, leveraging ZnO@MWCNTs/g-C_3N_4 nanosheets and CuO@CuPt nanocomposites for synergistic signal amplification and quenching, yielding an ultra-low LOD of 0.971 fg mL^{-1} ideal for portable food safety diagnostics [16]. Beyond single-mode detection, a portable ECL imaging test strip with dual-signal outputs was designed for AFB1 quantification in corn samples, utilizing Ru-PEI@SiO_2@Au nanospheres as luminescent probes. Notably, the ECL imaging mode achieved a 10-fold lower LOD than the standalone colorimetric mode, enabling on-site sensitive detection with robust practicality [67]. Besides, a zero-background BPE-ECL biosensor was fabricated for ochratoxin A (OTA) detection in beer, in which ZnCoN-C was employed to regulate driving potential, allowing smartphone-assisted ECL imaging with ultrahigh sensitivity and suppressed background interference [68]. Similarly, a dual-mode ECL-colorimetric system was constructed for deoxynivalenol (DON) monitoring by using COF@Luminol as emitters and Cu_xO nanorods as catalysts; the nanoconfinement effect significantly enhanced ECL efficiency, and smartphone-based imaging permitted label-free visual detection without nucleic acid amplification [69].

For antibiotic and pesticide residue detection, smartphone ECL systems have been tailored for high-specificity, field-deployable analysis. As illustrated in Figure 4, a dual-mode ECL-colorimetric sensing platform was innovated for tetracycline (TC) residue detection, utilizing CeO_2-porphyrin heterogeneous frameworks (CeO_2-POF) as a multifunctional material that integrated ECL luminophores, co-reaction accelerators, and peroxidase mimics in a single structure. The system achieved a LOD of 0.57 pM via smartphone for portable ECL food analysis, outperforming commercial ELISA kits in real-sample recovery performance [70]. A high-performance ECL aptasensor was also developed for diazinon (DZN) residues in vegetables, employing tris(2,2′-bipyridine)ruthenium(II) as a luminophore and PEI-Ag/Cu nanoclusters for signal enhancement. Its smartphone-readout system delivered a wide linear range of 1.0 to 10^6 pg mL^{-1} and a low LOD of 0.3 pg mL^{-1}, with exceptional specificity against common interfering pesticides, demonstrating its practical utility for on-site vegetable screening [71]. Complementing these, a low-cost smartphone-based ECL sensor was constructed for phenolic compounds (vanillic acid and p-coumaric acid) detection, leveraging the ECL quenching effect of phenols on the $Ru(bpy)_3^{2+}$/TPrA system at disposable screen-printed carbon electrodes, achieving LODs of 0.26 μM and 0.68 μM, respectively [72].

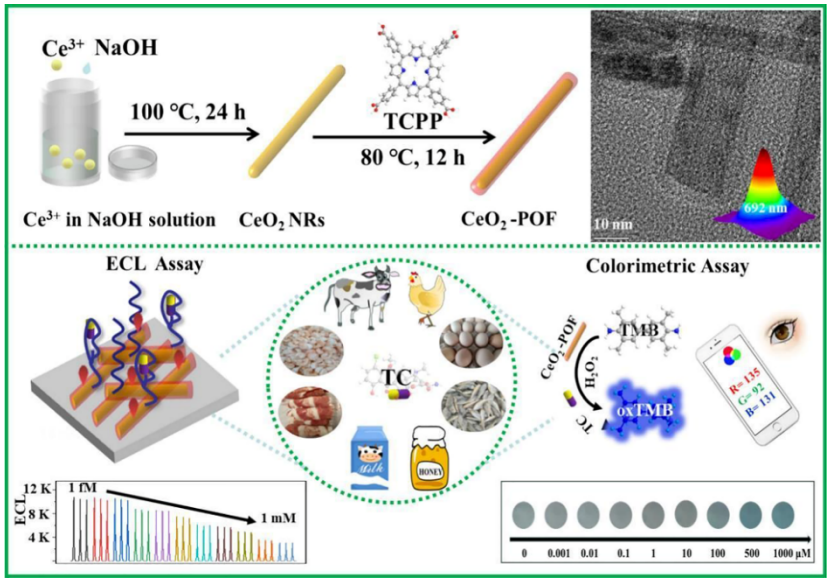

Figure 4. Schematic illustration of smartphone-based dual-mode ECL-colorimetric for detecting TC residues with CeO_2-POF as a multifunctional probe [70]. Copyright 2025, Elsevier.

4.3. Emerging and Interdisciplinary Applications

In addition to well-established bioanalysis, environmental monitoring, and food safety screening, smartphone-assisted ECL sensing has demonstrated remarkable versatility ranging from pathogenic monitoring and forensic identification to pharmaceutical evaluation, corrosion diagnosis, and fundamental luminescence research.

For microbial detection, Liu et al. established a visual ECL nanosensor relying on resonance energy transfer and surface plasmon-coupled luminescence for Shiga toxin-producing *Escherichia coli* gene detection employing BN QDs as luminophores and AuNPs as signal quenchers, and this smartphone-readable platform achieved a

detection limit of 0.3 pM within a linear range of 1 pM to 5 nM [73]. Complementing this, Li's group developed a graphene QDs-amplified ECL system for whole-cell *Escherichia coli* analysis based on the $Ru(bpy)_3^{2+}$/TPrA system, in which smartphone-controlled portable excitation and camera imaging were combined to realize quantitative detection over a range of 10 to 10^7 CFU mL^{-1}, showing great potential for point-of-care pathogenic screening [19].

Smartphone-coupled ECL devices also exhibit unique advantages in forensic science, anti-explosion screening, and security identification. For trace nitroaromatic explosive detection, Li et al. [74] developed a smartphone-based system using silica nanopore membrane-modified screen-printed electrodes, where the interpenetrating electron and ion channels within the nanopores enhanced $Ru(bpy)_3^{2+}$-based ECL signals. By smartphone-controlled USB-OTG stimulation and camera readout, combined with RGB/HSB/Gray multi-mode image analysis, the platform achieved sensitive detection across 10^{-7}–10^{-3} mg mL^{-1} with a LOD of 2.3×10^{-9} mg mL^{-1}, enabling reliable on-site explosive residue screening. Additionally, smartphone-integrated ECL imaging systems were established for high-resolution fingerprint mapping and biochemical sensing, enabling direct visualization of fingerprint grain details and sweat pores, while also supporting in situ analysis of exogenous substances including nicotine and trinitrotoluene (TNT) via ECL quenching, offering a rapid, non-invasive tool for forensic investigation and biometric recognition [75,76].

For pharmaceutical analysis and drug monitoring, a smartphone-based ECL-MIP sensor was developed using Ag^+@UiO-66-NH_2-decorated $CsPbBr_3$ perovskite nanomaterials as high-efficiency emitters for nitrofurazone detection. Powered by a rechargeable lithium-ion battery and combined with smartphone camera readout and machine-learning-assisted image analysis, the platform achieved a linear response from 0.5 nM to 100 μM with an ultra-low detection limit of 0.09 nM [77]. In addition, a smartphone-compatible ECL microscopy (SECLM) system was constructed for visual captopril imaging detection, utilizing Zn-MOF-encapsulated Ru-bpy complexes as ECL luminophores and MIP for selective recognition. The system demonstrated linear quantitation across 1–1×10^5 μM with a detection limit of 0.29 μM, providing a portable strategy for pharmacokinetic studies and drug toxicology research [78]. In summary, these applications highlight the significant potential of smartphone-based ECL sensing to meet customized, portable, and intelligent detection needs in interdisciplinary fields.

5. Conclusions and Perspectives

Smartphone-integrated ECL detection has emerged as a transformative portable analytical platform, synergistically combining the inherent high sensitivity of ECL with the ubiquity, advanced imaging capabilities, and computational intelligence of smartphones, effectively breaking the reliance on bulky centralized laboratory instrumentation for on-site, cost-effective analysis. Notably, traditional machine learning excels with low-dimensional spectral/electrochemical data, whereas deep learning is better suited to high-dimensional imaging tasks. While current deployments span bioanalysis, environmental monitoring, and food safety, several critical gaps remain to be addressed for practical translation, including insufficient system integration, signal instability, limited anti-interference capability, and a lack of generalizability in AI models. Future development is expected to focus on the design of highly integrated, miniaturized, and self-powered portable systems, driven by innovations in screen-printed electrodes, wireless energy supply, and compact optoelectrochemical modules. Lightweight deep learning models deployed directly on smartphones will facilitate real-time edge computing, enable multimodal signal fusion, and support adaptive noise reduction. Meanwhile, generalizable AI frameworks adaptable to diverse ECL systems and analytes are urgently needed to replace case-by-case model training. With continued innovation in functional materials, device architecture, and intelligent algorithms, smartphone ECL sensing is poised to achieve higher levels of sensitivity, stability, and analytical autonomy, paving the way for broader application prospects in POCT, food safety surveillance, and real-time environmental monitoring.

Author Contributions

F.D.: conceptualization, literature review, writing—original draft preparation, supervision, project administration; N.Y.: literature review, writing—review and editing, visualization; X.H.: literature review, writing—review and editing; F.X.: literature review, writing—review and editing; G.L.: supervision, writing—review and editing, project administration. All authors have read and agreed to the published version of the manuscript.

Funding

This research was supported by the National Natural Science Foundation of China (No. 22304058) and the Natural Science Foundation of Anhui Provincial Department of Education (No. 2024AH051690).

Conflicts of Interest

The authors declare no conflict of interest.

Use of AI and AI-Assisted Technologies

No AI tools were utilized for this paper.

References

1. Richter, M.M. Electrochemiluminescence (ECL). *Chem. Rev.* **2004**, *104*, 3003–3036. https://doi.org/10.1021/cr020373d.
2. Shi, B.N.; Ru, Z.Z.; Jia, D.H. Host-guest confinement in post-metallized COFs for enhanced electrochemiluminescence coupled with Y-shaped DNA amplification for microRNA-499 detection. *Biosens. Bioelectron.* **2026**, *304*, 118623.
3. Tang, X.H.; Peng, X.T.; Zhang, W.N. Ultrasensitive Electrochemiluminescence Nanoprobe for Early Screening and Early Diagnosis of Cervical Cancer. *Anal. Chem.* **2026**, *98*, 8550–8561.
4. Li, Y.M.; Dong, X.; Han, Y.J. Metal Defect-Mediated Adsorption-Catalytic Platform Drives Efficient Electrochemiluminescence Sensing. *Anal. Chem.* **2026**, *98*, 6139–6148.
5. Liu, G.Y.; Luo, Y.Q.; Cai, J.Y. Molecularly imprinted sensor based on dual emitting solid-state electrochemiluminescence of dinuclear Ru(II) complex for detecting tetracycline. *Sens. Actuators B* **2026**, *458*, 139856.
6. Sivakumar, R.; Lee, N.Y. Recent progress in smartphone-based techniques for food safety and the detection of heavy metal ions in environmental water. *Chemosphere* **2021**, *275*, 230096. https://doi.org/10.1016/j.chemosphere.2021.130096.
7. Fan, K.; Liu, W.; Miao, Y. Engineering Strategies for Advancing Optical Signal Outputs in Smartphone-Enabled Point-of-Care Diagnostics. *Adv. Intell. Syst.* **2023**, *5*, 2200285.
8. Xiang, X.X.; Sun, H.Y.; Chai, H.N. Research Advance on Smartphone-based Visual Biosensor in Point-of-Care Testing. *Chin. J. Anal. Chem.* **2024**, *52*, 145–156.
9. Dutta, C.; Citterio, D.; Nath, P. Present and future of smartphone-coupled chemiluminescence and electrochemiluminescence assays: A mini-review. *Analyst* **2025**, *150*, 1033–1047.
10. Rivera, E.C.; Swerdlow, J.J.; Summerscales, R.L. Data-Driven Modeling of Smartphone-Based Electrochemiluminescence Sensor Data Using Artificial Intelligence. *Sensors* **2020**, *20*, 625.
11. Zhang, Y.; Cui, Y.; Sun, M.; et al. Deep learning-assisted smartphone-based molecularly imprinted electrochemiluminescence detection sensing platform: Protable device and visual monitoring furosemide. *Biosens. Bioelectron.* **2022**, *209*, 114262. https://doi.org/10.1016/j.bios.2022.114262.
12. Lu, Z.; Dai, S.; Liu, T. Machine learning-assisted Te-CdS@Mn_3O_4 nano-enzyme induced self-enhanced molecularly imprinted ratiometric electrochemiluminescence sensor with smartphone for portable and visual monitoring of 2,4-D. *Biosens. Bioelectron.* **2023**, *222*, 114996.
13. Bhaiyya, M.; Rewatkar, P.; Pimpalkar, A.; et al. Deep Learning-Assisted Smartphone-Based Electrochemiluminescence Visual Monitoring Biosensor: A Fully Integrated Portable Platform. *Micromachines* **2024**, *15*, 1059. https://doi.org/10.3390/mi15081059.
14. Li, M.; Zhou, Z.; Tian, G.; et al. A machine-learning-integrated portable electrochemiluminescence sensing platform for the visualization and high-throughput immunoassays. *Talanta* **2025**, *287*, 127639. https://doi.org/10.1016/j.talanta.2025.127639.
15. Li, C.P.; Yang, Z.; Wang, J. Nanoconfinement-Enhanced Aggregation-Induced Electrochemiluminescence for Smartphone-Adopted Imaging Analysis of cTnI. *Adv. Funct. Mater.* **2025**, *35*, 2504380.
16. Xu, H.; Li, C.; Mao, R.; et al. Colorimetric and ECL dual-mode aptasensor for smartphone-based onsite sensitive detection of aflatoxin B1 in combination with ZnO@MWCNTs/ g-C_3N_4 nanosheets and CuO@CuPt nanocomposites. *Biosens. Bioelectron.* **2024**, *262*, 116569. https://doi.org/10.2139/ssrn.4805530.
17. Li, F.; Xi, Y.C.; Jiang, J.M. O-Fluorobenzoic Acid-Mediated Construction of Porous Graphitic Carbon Nitride with Nitrogen Defects for Multicolor Electrochemiluminescence Imaging Sensing. *Anal. Chem.* **2022**, *94*, 9306–9315.
18. Li, F.; Peng, H.; Shen, N.T.; et al. Electrochemiluminescence in Graphitic Carbon Nitride Decorated with Silver Nanoparticles for Dopamine Determination Using Machine Learning. *ACS Appl. Mater. Interfaces* **2024**, *16*, 27767–27777. https://doi.org/10.1021/acsami.4c03996.
19. Li, S.; Liu, J.; Chen, Z. Electrogenerated chemiluminescence on smartphone with graphene quantum dots nanocomposites for Escherichia Coli detection. *Sens. Actuators B* **2019**, *297*, 126811.
20. Gao, W.; Muzyka, K.; Ma, X.; et al. A single-electrode electrochemical system for multiplex electrochemiluminescence analysis based on a resistance induced potential difference. *Chem. Sci.* **2018**, *9*, 3911–3916. https://doi.org/10.1039/c8sc00410b.
21. Du, F.; Dong, Z.; Guan, Y. Single-Electrode Electrochemical System for the Visual and High-Throughput Electrochemiluminescence Immunoassay. *Anal. Chem.* **2022**, *94*, 2189–2194.
22. Eticha, T.; Zhu, M.; Dong, Z. Single-electrode electrochemiluminescence immunosensor for multiplex detection of Aquaporin-4 antibody using metal-organic gels as coreactant. *Biosens. Bioelectron.* **2025**, *272*, 117128.

23. Guo, M.; Pan, Y.; Du, D.; et al. Single-electrode electrochemiluminescence immunoarray combined with smartphone for high-throughput detection of heart-type fatty acid binding protein. *Microchem. J.* **2025**, *212*, 113249. https://doi.org/10.1016/j.microc.2025.113249.
24. Ning, Y.; Du, Y.; Guan, Y. Single-Electrode Electrochemiluminescence System for High-Throughput Visual Analysis of Chloramphenicol. *Anal. Chem.* **2025**, *97*, 18815–18825.
25. Dong, Y.; Fu, B.; Wu, H. Single-Electrode High-Throughput 12-Well Array Electrochemiluminescence Imaging Sensor for Portable Parallel Dual-Color Analysis of Dual Breast Cancer Susceptibility Genes. *Anal. Chem.* **2026**, *98*, 5593–5602.
26. Xu, W.; Fu, K.; Ma, C.; et al. Closed bipolar electrode-enabled dual-cell electrochromic detectors for chemical sensing. *Analyst* **2016**, *141*, 6018–6024.
27. Rahn, K.L.; Rhoades, T.D.; Anand, R.K. Alternating Current Voltammetry at a Bipolar Electrode with Smartphone Luminescence Imaging for Point-of-Need Sensing. *ChemElectroChem* **2020**, *7*, 1172–1181. https://doi.org/10.1002/celc.202000079.
28. Zhang, R.; Dai, D.; Cao, Y. A portable smartphone-based electrochemiluminescence device integrated with bipolar electrode detection chip for multi-target respiratory pathogen detection. *Biosens. Bioelectron.* **2025**, *288*, 117783.
29. Phujeenaphun, A.; Tinala, C.; Jakmunee, J.; et al. Bipolar electrochemiluminescence on a low-cost and flexible porous laminated-gold leaf electrode for determination of hydrogen peroxide, glucose and uric acid. *Talanta* **2026**, *298*, 128992. https://doi.org/10.1016/j.talanta.2025.128992.
30. Yao, Y.; Li, H.; Wang, D.; et al. An electrochemiluminescence cloth-based biosensor with smartphone-based imaging for detection of lactate in saliva. *Analyst* **2017**, *142*, 3715–3724.
31. Eynaki, H.; Kiani, M.A.; Golmohammadi, H. Nanopaper-based screen-printed electrodes: A hybrid sensing bioplatform for dual opto-electrochemical sensing applications. *Nanoscale* **2020**, *12*, 18409–18417. https://doi.org/10.1039/d0nr03505j.
32. Tamiya, E.; Osaki, S.; Nagai, H. Wireless electrochemiluminescent biosensors: Powering innovation with smartphone technology. *Biosens. Bioelectron.* **2024**, *252*, 116083.
33. Liu, H.; Hussain, A.; Zholudov, Y.T. Self-Powered Electrochemiluminescence for Imaging the Corrosion of Protective Coating of Metal and Quantitative Analysis. *Angew. Chem. Int. Ed.* **2024**, *63*, 202411764.
34. Escobedo, P.; Erenas, M.M.; Martinez-Olmos, A. General-purpose passive wireless point-of-care platform based on smartphone. *Biosens. Bioelectron.* **2019**, *141*, 111360.
35. Rivera, E.C.; Summerscales, R.L.; Uppala, P.P.T.; et al. Electrochemiluminescence Mechanisms Investigated with Smartphone-Based Sensor Data Modeling, Parameter Estimation and Sensitivity Analysis. *ChemistryOpen* **2020**, *9*, 854–863. https://doi.org/10.1002/open.202000165.
36. Rodriguez Muina, S.; Gajjala, R.K.R.; Fernandez Martin, E. Gamma Correction and Color Space Transformations for Quantitative Analysis of Electrochemiluminescence Images Using Smartphone Cameras. *Chem. Biomed. Imaging* **2025**, *3*, 767–778. https://doi.org/10.1021/cbmi.5c00056.s001.
37. Firoozbakhtian, A.; Hosseini, M.; Sheikholeslami, M.N. Detection of COVID-19: A Smartphone-Based Machine-Learning-Assisted ECL Immunoassay Approach with the Ability of RT-PCR CT Value Prediction. *Anal. Chem.* **2022**, *94*, 16361–16368.
38. Kumar, A.; Jain, D.; Bahuguna, J. Machine learning assisted and smartphone integrated homogeneous electrochemiluminescence biosensor platform for sample to answer detection of various human metabolites. *Biosens. Bioelectron.* **2023**, *238*, 115582.
39. Lu, Z.; Qin, J.; Wu, C.; et al. Dual-channel MIRECL portable devices with impedance effect coupled smartphone and machine learning system for tyramine identification and quantification. *Food Chem.* **2023**, *429*, 136920. https://doi.org/10.1016/j.foodchem.2023.136920.
40. Lu, Z.; Gong, Y.; Shen, C.; et al. Portable, intelligent MIECL sensing platform for ciprofloxacin detection using a fast convolutional neural networks-assisted Tb@Lu_2O_3 nanoemitter. *Food Chem.* **2024**, *444*, 138656. https://doi.org/10.1016/j.foodchem.2024.138656.
41. Wang, Y.; Dai, S.; Liu, T. Sulfur vacancy defects mediated CdZnTeS@BC heterojunction: Artificial intelligence-assisted self-enhanced electrochemiluminescence molecularly imprinted sensing of CTC. *Biosens. Bioelectron.* **2024**, *248*, 115941.
42. Gong, Y.; Yong, K.; Zhu, W. Vacancy mediated CdZnS/SnIn4S8 heterojunction coupling Co_3O_4/CuO nanozymes: Artificial intelligence assisted ratiometric electrochemiluminescence sensing of tetracycline. *Electrochimica. Acta* **2025**, *521*, 145881.
43. Zhu, L.; Fu, W.; Chen, J. A fully integrated and handheld electrochemiluminescence device for detection of dopamine in bio-samples. *Sens. Actuators B* **2022**, *366*, 131972.
44. Bhaiyya, M.; Kulkarni, M.B.; Pattnaik, P.K.; et al. Internet of things-enabled photomultiplier tube- and smartphone-based electrochemiluminescence platform to detect choline and dopamine using 3D-printed closed bipolar electrodes. *Luminescence* **2022**, *37*, 357–365. https://doi.org/10.1002/bio.4179.
45. Pan, J.; Zhang, R.; Xia, S.; et al. High-throughput point-of-care testing using the smartphone-based, cloud computing-enabled ECL analyzer and single ITO electrode-based sensing chips. *Microchem. J.* **2025**, *209*, 112707. https://doi.org/10.1016/j.microc.2025.112707.

46. Calabria, D.; Lazzarini, E.; Pace, A. Smartphone-based 3D-printed electrochemiluminescence enzyme biosensor for reagentless glucose quantification in real matrices. *Biosens. Bioelectron.* **2023**, *227*, 115146.
47. Wang, M.; Wei, M.; Su, W. Electrochemiluminescence-colorimetric dual-mode biosensor based on CeO_2:Eu^{3+} nanozyme amplification for the detection of glucose. *Biosens. Bioelectron.* **2026**, *291*, 118027.
48. Nie, Y.; Liu, Y.; Zhang, Q. Novel coreactant modifier-based amplified electrochemiluminescence sensing method for point-of-care diagnostics of galactose. *Biosens. Bioelectron.* **2019**, *138*, 111318.
49. Nie, Y.; Liu, Y.; Zhang, Q. Fe_3O_4 NP@ZIF-8/MoS_2 QD-based electrochemiluminescence with nanosurface energy transfer strategy for point-of-care determination of ATP. *Anal. Chim. Acta* **2020**, *1127*, 190–197.
50. Zhang, X.; Nie, Y.; Zhang, Q. A novell-cysteine regulated polydopamine nanoparticle-based electrochemiluminescence image application. *J. Mater. Chem. C* **2020**, *8*, 8592–8600.
51. Wu, Y.; Qin, D.; Luo, Z. Construction of a smartphone-based electrochemiluminescence imaging device to guide the improvement of sensing performance via surface regulation. *Sens. Actuators B* **2023**, *389*, 133885.
52. Wu, Y.; Hu, S.; Xu, L. Smartphone-based molecular imprinting electrochemiluminescence microscope for non-invasive alpha-fetoprotein visual quantitation. *Anal. Chim. Acta* **2026**, *1383*, 344922.
53. Shi, S.S.; Li, X.J.; Ma, R.N.; et al. A smartphone-based electrochemical POCT for CEA based on signal amplification of Zr_6MOFs. *Lab. Chip* **2024**, *24*, 367–374. https://doi.org/10.1039/d3lc00748k.
54. Arab, N.; Hosseini, M.; Xu, G. Engineering a self-sufficient ECL system: Oxygen-vacancy-driven O_2 generation and nanozyme confinement for bioanalysis. *Biosens. Bioelectron.* **2026**, *301*, 118491.
55. Nie, W.; Zhang, R.; Hu, C. A self-enhanced electrochemiluminescence array chip for portable label-free detection of SARS-CoV-2 nucleocapsid protein with smartphone. *Biosens. Bioelectron.* **2023**, *240*, 115662.
56. Liu, Y.; Jiang, K.; Nie, Y. A visual electrochemiluminescence biosensor based on CuInZnS quantum dots for superoxide dismutase detection. *Anal. Bioanal. Chem.* **2020**, *412*, 1893–1899.
57. Liu, Y.; Wang, M.; Nie, Y. Sulfur Regulated Boron Nitride Quantum Dots Electrochemiluminescence with Amplified Surface Plasmon Coupling Strategy for BRAF Gene Detection. *Anal. Chem.* **2019**, *91*, 6250–6258.
58. Nie, Y.; Zhang, X.; Zhang, Q. A novel high efficient electrochemiluminescence sensor based on reductive Cu(I) particles catalyzed Zn-doped MoS2 QDs for HPV 16 DNA determination. *Biosens. Bioelectron.* **2020**, *160*, 112217.
59. Zhang, X.; Nie, Y.; Zhang, Q. Polydopamine nanoparticles@MoS_2 nanosheet aerogel-based ECL sensing system for MiRNA-126 detection. *Chem. Eng. J.* **2021**, *411*, 128428.
60. Zheng, K.; Pan, J.; Yu, Z.; et al. A smartphone-assisted electrochemiluminescent detection of miRNA-21 in situ using $Ru(bpy)_3^{2+}$@MOF. *Talanta* **2024**, *268*, 125310. https://doi.org/10.1016/j.talanta.2023.125310.
61. Zheng, K.; Zheng, Q.; Mu, X.; et al. A smartphone-assisted electrochemiluminescent biosensor for highly sensitive detection of miRNA-21 based on $Ru(bpy)_2(L)^{4+}$@MOF-5. *Microchim. Acta* **2024**, *191*, 596. https://doi.org/10.1007/s00604-024-06675-9.
62. Khoshfetrat, S.M.; Dorraji, P.S.; Shayan, M. Smartphone-Based Electrochemiluminescence for Visual Simultaneous Detection of RASSF1A and SLC5A8 Tumor Suppressor Gene Methylation in Thyroid Cancer Patient Plasma. *Anal. Chem.* **2022**, *94*, 8005–8013.
63. Sun, Y.; Wei, M.; Liu, R.; et al. A smartphone-based ratiometric fluorescent device for field analysis of soluble copper in river water using carbon quantum dots as luminophore. *Talanta* **2019**, *194*, 452–460. https://doi.org/10.1016/j.talanta.2018.10.019.
64. Ma, Y.; Yu, Y.; Mu, X.; et al. Enzyme-induced multicolor colorimetric and electrochemiluminescence sensor with a smartphone for visual and selective detection of Hg^{2+}. *J. Hazard. Mater.* **2021**, *415*, 125538. https://doi.org/10.1016/j.jhazmat.2021.125538.
65. Cai, L.; Hao, W.; Cao, Y. Near-infrared electrochemiluminescence/smart visual dual-channel sensor based on magnetic derivative and microchip of terbium-based double-ligand MOG for detecting nitrofurazone and Cr(VI). *Chem. Eng. J.* **2025**, *505*, 159385.
66. Khoshfetrat, S.M.; Bagheri, H.; Mehrgardi, M.A. Visual electrochemiluminescence biosensing of aflatoxin M1 based on luminol-functionalized, silver nanoparticle-decorated graphene oxide. *Biosens. Bioelectron.* **2018**, *100*, 382–388.
67. Chen, M.M.; Zhang, M.L.; Song, X. Smartphone-assisted electrochemiluminescence imaging test strips towards dual-signal visualized and sensitive monitoring of aflatoxin B1 in corn samples. *Chin. Chem. Lett.* **2025**, *36*, 109785.
68. Li, H.; Cai, Q.; Li, P. Zero-Background Dual-Mode Closed Bipolar Electrode Electrochemiluminescence Biosensor Based on ZnCoN-C Potential Regulation for Ultrasensitive Detection of Ochratoxin A. *Anal. Chem.* **2024**, *96*, 13987–13995.
69. Cai, Q.; Li, H.; Shi, A. Nanoconfinement Effect and CuxO Nanorod Electrocatalysts Enhance COF@Lu Electrochemiluminescence for Biosensing. *Anal. Chem.* **2026**, *98*, 1306–1315.
70. Shi, X.; Cao, Y.; Cong, L.; et al. Novel nanoceria in situ-derived porphyrin heterostructure enhanced electrochemiluminescent and colorimetric dual-mode detection of tetracycline residue in foods. *Food Chem.* **2025**, *485*, 144459. https://doi.org/10.1016/j.foodchem.2025.144459.
71. Fang, M.; Liu, W.; Wang, Y. High-performance electrochemiluminescence aptasensing platform for diazinon based on smartphone imaging and PEI-Ag/Cu nanocluster-enhanced luminescence. *Microchim. Acta* **2025**, *193*, 13.
72. Rivera, E.C.; Taylor, J.W.; Summerscales, R.L.; et al. Quenching Behavior of the Electrochemiluminescence of

Ru(bpy)32+/TPrA System by Phenols on a Smartphone-Based Sensor. *ChemistryOpen* **2021**, *10*, 842–847. https://doi.org/10.1002/open.202100151.

73. Liu, Y.; Chen, X.; Wang, M.; et al. A visual electrochemiluminescence resonance energy transfer/surface plasmon coupled electrochemiluminescence nanosensor for Shiga toxin-producing Escherichia coli detection. *Green. Chem.* **2018**, *20*, 5520–5527. https://doi.org/10.1039/c8gc03010c.
74. Li, S.; Zhang, D.; Liu, J. Electrochemiluminescence on smartphone with silica nanopores membrane modified electrodes for nitroaromatic explosives detection. *Biosens. Bioelectron.* **2019**, *129*, 284–291.
75. Li, S.; Lu, Y.; Liu, L. Fingerprints mapping and biochemical sensing on smartphone by electrochemiluminescence. *Sens. Actuators. B* **2019**, *285*, 34–41.
76. Sornambigai, M.; Jaijanarathanan, L.; Hansda, S.; et al. Study of highly stable electrochemiluminescence from $[Ru(bpy)_3]^{2+}$/dicyclohexylamine and its application in visualizing sebaceous fingerprint. *Chem. Commun.* **2022**, *58*, 7305–7308. https://doi.org/10.1039/d2cc01929a.
77. Liu, T.; He, J.; Lu, Z. A visual electrochemiluminescence molecularly imprinted sensor with Ag+@UiO-66-NH2 decorated CsPbBr3 perovskite based on smartphone for point-of-care detection of nitrofurazone. *Chem. Eng. J.* **2022**, *429*, 132462.
78. Wu, Y.; Qin, D.; Yang, J.; et al. Emitter-embedded metal-organic framework combined with molecularly-imprinted electrochemiluminescence microscopy for drug imaging detection. *Microchem. J.* **2024**, *207*, 112167. https://doi.org/10.1016/j.microc.2024.112167.